Spin-state splittings, highest-occupied-molecular-orbital and lowest-unoccupied-molecular-orbital energies, and chemical hardness

Erin R. Johnson,[1,2] Weitao Yang,[2,a)] and Ernest R. Davidson[3]
[1]*School of Natural Sciences, University of California, Merced, Merced, California 95343, USA*
[2]*Department of Chemistry, Duke University, Durham, North Carolina 27708, USA*
[3]*Department of Chemistry, University of Washington, Seattle, Washington 98195, USA*

(Received 21 June 2010; accepted 15 September 2010; published online 26 October 2010)

It is known that the exact density functional must give ground-state energies that are piecewise linear as a function of electron number. In this work we prove that this is also true for the lowest-energy excited states of different spin or spatial symmetry. This has three important consequences for chemical applications: the ground state of a molecule must correspond to the state with the maximum highest-occupied-molecular-orbital energy, minimum lowest-unoccupied-molecular-orbital energy, and maximum chemical hardness. The beryllium, carbon, and vanadium atoms, as well as the CH_2 and C_3H_3 molecules are considered as illustrative examples. Our result also directly and rigorously connects the ionization potential and electron affinity to the stability of spin states. © *2010 American Institute of Physics*. [doi:10.1063/1.3497190]

I. INTRODUCTION

In the vast majority of organic molecules, the electronic ground state is a singlet, such that atoms obey the "octet" occupation rule. However, electron-deficient molecules are occasionally encountered and there is no general rule to predict their most-stable electronic configuration. A simple example is the case of carbenes in which a carbon atom participates in two chemical bonds and has two additional electrons not involved in bonding. Carbenes can exist in either a singlet or triplet state, which are generally quite close in energy.[1,2] More commonly, transition-metal compounds often have several low-energy electronic states. This has wide-reaching consequences and determines reactivity in inorganic chemistry.[3] Knowledge of the most-stable spin state is important in mechanistic studies of inorganic catalysts and particularly of enzymatic catalysts where the active sites contain transition metals.

The prediction of the correct ground state of inorganic molecules is an extremely challenging theoretical problem often requiring highly correlated, and even multireference, wave function theory techniques.[4] The more efficient Hartree–Fock or density-functional theory (DFT) methods are unreliable and tend to give systematic errors. Hartree–Fock theory, which accounts for electron exchange exactly, but neglects correlation between opposite-spin electrons, always favors high-spin configurations. Conversely, pure density functionals, which give approximate treatments of both exchange and correlation effects, generally favor low-spin states. Examples are iron carbonyl and iron porphyrins.[3,5]

Given the computational difficulty of obtaining accurate spin-state energy splittings, simple rules for predicting ground-state configurations can provide valuable insight. One such is Walsh's rule, which is that the ground state of a molecule best stabilizes its highest occupied molecular orbital (HOMO).[6] However, this conclusion was drawn from studies of molecular geometries and not different electronic states. Walsh's rule has been put on a firmer theoretical footing by Coulson and Deb[7] and by March.[8]

Another useful rule is the principle of maximum hardness, which is that the state with the largest chemical hardness value is most stable.[9,10] The chemical hardness (η) is equal to the difference in ionization potential (I) and electron affinity (A)

$$\eta = \tfrac{1}{2}(I - A). \tag{1}$$

There is considerable evidence for the maximum-hardness principle,[9] such as studies of small molecules[11] and of metal clusters.[12] The maximum-hardness principle has been proven within a density-functional framework for the ground electronic state.[13,14] However, its validity for distinguishing between different electronic states has not been proven and this appears unlikely on first inspection since DFT is a ground-state theory. Such a proof is needed to rigorously apply the maximum-hardness principle to different spin states.

Calculation of hardness can be made through the chemical potential,[15,16] which is defined as the derivative of the total energy with respect to particle number when the external potential is fixed,

$$\mu(N) = \left(\frac{\partial E_v(N)}{\partial N}\right)_v. \tag{2}$$

The derivative discontinuity of $E_v(N)$ with respect to electron number at an integer N_0 gives the energy gap or the hardness. As a consequence of the linearity condition,[17] μ is a constant between the integers and has a derivative discontinuity at the integers

a)Electronic mail: weitao.yang@duke.edu.

$$\mu(N) = \begin{cases} -I(N_0) = E(N_0) - E(N_0 - 1) & \text{if } N_0 - 1 < N < N_0 \\ -A(N_0) = E(N_0 + 1) - E(N_0) & \text{if } N_0 < N < N_0 + 1, \end{cases} \tag{3}$$

where $I(N_0)$ is the ionization potential of the N_0-electron system and $A(N_0)$ is its electron affinity. This is a generalization of the usual integer expression and can be evaluated for finite-size systems, but not for bulk systems. That μ is discontinuous at the integers is understandable because only one electron can occupy a given spin orbital; additional electrons must be placed in higher-energy orbitals.

In all calculations with fractional number of electrons, we follow Janak[18] and extend the noninteracting Kohn–Sham first-order reduced density matrix to fractional charge δ by the definition

$$\rho_s(\mathbf{r}', \mathbf{r}) = \sum_i n_i \phi_i(\mathbf{r}') \phi_i^*(\mathbf{r}), \tag{4}$$

where $n_i = 1$ for $i < \mathrm{f}$, $n_i = \delta$ for $i = \mathrm{f}$, and $n_i = 0$, for $i > \mathrm{f}$, and f is the index for the frontier orbital. This density matrix is an ensemble of single Slater determinants. This agrees with Kohn–Sham (KS) for integer charges and provides a simple linear interpolation for fractional charges. The energy functional evaluated for this ensemble density matrix is then the energy of the corresponding fractional system.

There are two ways to carry out a DFT calculation: with the one-electron orbitals $\{|\phi_i\rangle\}$ as the eigenstates of a one-electron local potential $v_s(\mathbf{r})$

$$\left(-\tfrac{1}{2}\nabla^2 + v_s(\mathbf{r})\right)|\phi_i\rangle = \varepsilon_i|\phi_i\rangle, \tag{5}$$

or a nonlocal potential $v_s^{\mathrm{NL}}(\mathbf{r}, \mathbf{r}')$

$$\left(-\tfrac{1}{2}\nabla^2 + v_s^{\mathrm{NL}}(\mathbf{r}, \mathbf{r}')\right)|\phi_i\rangle = \varepsilon_i^{\mathrm{GKS}}|\phi_i\rangle. \tag{6}$$

The former is the original Kohn–Sham method with corresponding eigenvalues $\{\varepsilon_i\}$ (or equivalently $\{\varepsilon_i^{\mathrm{KS}}\}$). The latter has been called the Hartree–Fock–Kohn–Sham[19] or the generalized Kohn–Sham (GKS) method,[20] with corresponding eigenvalues $\{\varepsilon_i^{\mathrm{GKS}}\}$. Cohen *et al.*[21] recently developed the formula for evaluating the chemical potential in DFT calculations by evaluating the derivative $(\partial E_v/\partial N)_v$ directly from the quantities of the noninteracting reference KS or GKS system. These are based on the potential functional theory formulation of DFT.[22] Their results lead to the following simple equations:

$$\mu(N) = \varepsilon_f = \begin{cases} \varepsilon_{\mathrm{HOMO}}(N_0) & \text{if } N_0 - 1 < N < N_0 \\ \varepsilon_{\mathrm{LUMO}}(N_0) & \text{if } N_0 < N < N_0 + 1, \end{cases} \tag{7}$$

where ε_f is the eigenvalue of the frontier orbital, $\varepsilon_{\mathrm{HOMO}}(N_0) = \varepsilon_{N_0}(N_0)$ and $\varepsilon_{\mathrm{LUMO}}(N_0) = \varepsilon_{N_0+1}(N_0)$. This definition is introduced to connect the chemical potential to orbital eigenvalues, as well as the usual expression in terms of ionization potential and electron affinity. The definition of the chemical potential in Eq. (7) is identical to Eq. (3) for the exact functional, which gives energies that are piecewise linear as a function of fractional electron number. This is not the case for approximate functionals, such as the local density approximation (LDA) and generalized gradient approximations (GGAs). However, the two definitions should be approximately equal at Slater's transition state, where one half of an electron has been added or removed $(N = N_0 \pm \frac{1}{2})$.

The eigenvalues in Eq. (7) should be interpreted as the KS eigenvalues when the exchange-correlation energy functional used is an explicit and continuous functional of electron density, such as the local density approximation or generalized gradient approximations. They should be interpreted as the GKS eigenvalues when the exchange-correlation energy functional is an explicit and continuous functional of electron density matrix (sometime called orbital functionals), such as Hartree–Fock or hybrid approximations.[23,24] Note that for such functionals, the chemical potential is *not* equal to the eigenvalue of the frontier orbital in the optimized effective potential calculations.[25]

Provided the DFT calculations are performed as described above, the chemical hardness is the second derivative of the energy with respect to the number of electrons N at constant external (nuclear) potential, v (Refs. 10 and 14)

$$\eta = \left(\frac{\partial^2 E}{\partial N^2}\right)_v = \tfrac{1}{2}[(E(N-1) - E(N)) - (E(N) - E(N+1))]$$
$$= \tfrac{1}{2}(I - A). \tag{8}$$

Consideration of this form provides a clear route to proving the maximum-hardness principle for different electronic states. The behavior of density functionals for fractional electron numbers has been the subject of much recent study, providing new understanding of the errors inherent in most commonly used functionals.[21,26–29]

The exact density functional should give energies that are piecewise linear between integer electron numbers. This was originally proven by Perdew *et al.*[17] and later reformulated by Yang *et al.*[30] In this work, we extend the derivation to the lowest-energy states of each spin and spatial symmetry. We will show that the most-stable electronic configuration of a molecule must have the lowest HOMO energy, highest lowest-unoccupied-molecular-orbital (LUMO) energy, maximum HOMO-LUMO gap, and maximum chemical hardness. These constraints, which are natural consequences of the piecewise linearity of exact density-functional energies, connect the ionization potential and electron affinity to the stability of spin states. We consider five practical examples of density-functional calculations: the beryllium cation, the carbon and vanadium atoms, and the CH_2 and C_3H_3 molecules, all of which have low-lying excited states.

II. THEORY

In this section, we outline an intuitive proof of straight-line behavior for molecular energies as a function of electron number. This will be formalized in Sec. III. The key is to recognize the equivalence between an isolated atom or molecule with fractional electron number $N \pm \delta$ and a collection of equivalent atoms or molecules, which are separated from each other by an infinite distance and, hence, are noninteracting. In this combined system, some fraction δ of the atoms or molecules possesses $N \pm 1$ electrons and the remaining fraction $1 - \delta$ has N electrons.

For a large system with k molecules all in the N-electron ground state, consider how the energy changes as electrons are added or removed. A single electron added (or removed) will give a system with a single molecule in the $N+1$ (or $N-1$) electron ground-state and all other molecules remaining in the N-electron ground state. After ionization, it is possible to write k different wave functions with one molecule ionized and the rest neutral. Each of these is a valid wave function and so is the normalized linear combination over all possible ion positions. This ensemble wave function will necessarily have the same energy $(k-1)E(N)+E(N\pm1)$, but a different (ensemble average) density.

Going to DFT, the densities from each of the k possible wave functions will also give degenerate energies of $(k-1)E(N)+E(N\pm1)$. With the exact functional, this same energy must be obtained using the ensemble average density as well. This density can be constructed as a sum over each of the k molecules using fractional occupancies $\Sigma_{i=1}^{k}(1-1/k)\rho_i(N)+(1/k)\rho_i(N\pm1)$. Since the molecules are indistinguishable, the energy from each of these densities is $(1/k)E_{\text{total}}=(1-1/k)E(N)+(1/k)E(N\pm1)$, which is a linear combination of the integer values.

The addition (or removal) of electrons can be carried out sequentially, until all the molecules are in the $N+1$ (or $N-1$) ground state. Thus, the energy should vary linearly between that of the N-electron ground state and that of the $N+1$ (or $N-1$) electron state. Addition (or removal) of subsequent electrons will cause appearance of a new $N+2$ (or $N-2$) state, and the energy will now vary linearly between the values for the $N+1$ and $N+2$ (or $N-1$ and $N-2$) electron states. Our earlier argument holds for each successive ionization from the ensemble of k molecules. Therefore, recognizing the connection between the ensemble average density and a molecule with fractional occupancy, the molecular electronic energy must be piecewise linear as a function of electron number.

In the above argument, we assumed that the molecules were initially in the N-electron ground state and moreover that the addition or removal of electrons resulted in the $N+1$ (or $N-1$) electron ground states. However, the assumption of ground-state electron configurations is not strictly necessary. Electrons can be consistently added (or removed) from each molecule to give a collection of molecules all in a higher-energy $N+1$ (or $N-1$) electron excited state, assuming that it is stable and does not autoionize. If all the molecules in the system vary by one-electron processes between the same N-electron and $N+1$ (or $N-1$) electron states, be they ground or excited states, the energy of the system must still vary linearly throughout. Therefore, an exact density functional must give energies that are piecewise linear as a function of electron number for any molecule. This is applicable not only to the ground state, but also the lowest-energy excited states with a different net spin or different spatial symmetry. The condition of differing spin or spatial symmetry from the ground-state is necessary to impose an additional constraint on the electron density. A more rigorous, formal proof of this result is shown in Sec. III.

An interesting implication of the constraint of piecewise-linear energies is, for the exact functional, the total electronic energy is a sum of the HOMO eigenvalues of the molecule with $1,2,3\ldots,N$ electrons. Note that this is *not* the same as the sum of the eigenvalues for the N-electron species, however, since the lower-energy eigenvalues will no longer be constant upon addition of further electrons.

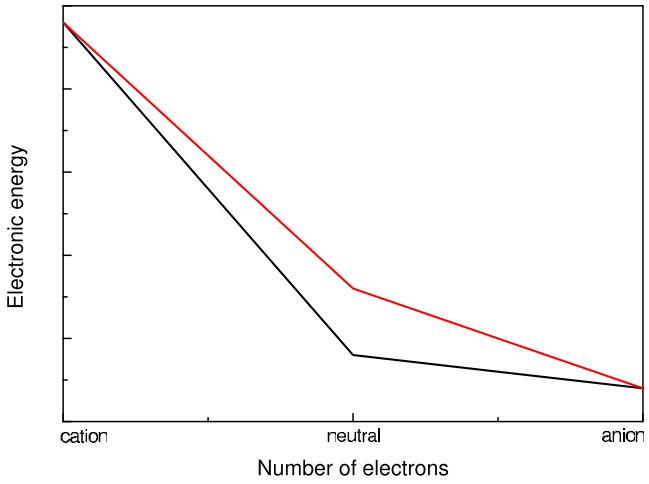

FIG. 1. Sketch of the electronic energies of a two-state system as a function of the number of electrons.

An important chemical consequence is that the exact LUMO or HOMO energies of an N-electron molecule must remain constant as an electron is added or removed, respectively. Also, the vertical ionization potential is identically equal to the negative HOMO eigenvalue of the neutral molecule and the electron affinity is equal to the LUMO eigenvalue.[27] Note that this requires Hartree–Fock or generalized Kohn–Sham eigenvalues and will not apply to eigenvalues calculated from an optimized effective potential.[27] Therefore, assuming a constant geometry, the chemical hardness is directly related to the HOMO-LUMO energy gap

$$\eta=\tfrac{1}{2}(\varepsilon_{\text{LUMO}}-\varepsilon_{\text{HOMO}}). \tag{9}$$

Consider a molecule with two possible low-lying N-electron states, both of which can be reached by addition or removal of a single electron from the *same* cation and anion states. This situation is illustrated by the $E(N)$ curves sketched in Fig. 1. A similar plot is shown by Ayers in Ref. 14. Assume that there is molecular symmetry and we are discussing the lowest state of two different irreducible representations. Let us label these two states of the N-electron system as A and B with energies $E(N,A)$ and $E(N,B)$, such that $E(N,B)$ is the lower of the two. We can also label the highest occupied orbital energy of each symmetry in the neutral molecules by $e_{\text{HOMO}}(N,A)$ and $e_{\text{HOMO}}(N,B)$. Then we can write the energies of both states of the N-electron system in terms of the cation energies and orbital eigenvaules

$$E(N,A)=E(N-1)+e_{\text{HOMO}}(N,A), \tag{10}$$

$$E(N,B)=E(N-1)+e_{\text{HOMO}}(N,B). \tag{11}$$

We can also write the energies of both states of the N-electron system in terms of the anion energies and orbital eigenvaules

$$E(N,A) = E(N+1) - e_{\mathrm{LUMO}}(N,A), \tag{12}$$

$$E(N,B) = E(N+1) - e_{\mathrm{LUMO}}(N,B). \tag{13}$$

Let us start from the shared cation state at the left side of the plot in Fig. 1. Equations (10) and (11) mean that, for each of the two possible neutral states, the energy will equal the cation energy plus the slope of the $E(N)$ curve leading from the cation to the neutral. This slope is equal to the HOMO eigenvalue of the neutral atom or molecule, which gives $E(N)=E(N-1)+\varepsilon_{\mathrm{HOMO}}(N)$. The energy difference between the two neutral states is thus equal to the difference between their HOMO eigenvalues. Therefore, we conclude that the state with the most-stable HOMO must have the lowest energy. This is equivalent to Walsh's rule that the ground state best stabilizes the HOMO,[6] but at fixed geometry.

Now start from the shared anion state at the right side of the plot in Fig. 1. From Eqs. (12) and (13), the energy of each neutral state will equal the anion energy minus the slope of the $E(N)$ curve leading from the anion to the neutral. This slope is equal to the LUMO eigenvalue of the neutral atom or molecule [$e_{\mathrm{LUMO}}(N,A)$ for state A and $e_{\mathrm{LUMO}}(N,B)$ for state B], which gives $E(N)=E(N+1)-\varepsilon_{\mathrm{LUMO}}(N)$. The energy difference between the two neutral states is now equal to the difference between their LUMO eigenvalues. Therefore, the state with the higher-lying LUMO must have the lowest energy.

Combining these last two results, the most-stable state has the lowest HOMO and highest LUMO, which implies the largest HOMO-LUMO gap. To show this more rigorously, recall that $E(N,B)<E(N,A)$ and substitute the results from Eqs. (10) and (13) to give

$$E(N+1) - e_{\mathrm{LUMO}}(N,B) < E(N-1) + e_{\mathrm{HOMO}}(N,A). \tag{14}$$

This can be rewritten as

$$E(N+1) - E(N-1) < e_{\mathrm{LUMO}}(N,B) + e_{\mathrm{HOMO}}(N,A). \tag{15}$$

Similarly, substituting the results from Eqs. (11) and (12) gives

$$E(N+1) - E(N-1) > e_{\mathrm{HOMO}}(N,B) + e_{\mathrm{LUMO}}(N,A). \tag{16}$$

Combining these gives

$$e_{\mathrm{LUMO}}(N,B) - e_{\mathrm{HOMO}}(N,B) > e_{\mathrm{LUMO}}(N,A) - e_{\mathrm{HOMO}}(N,A), \tag{17}$$

which for $E(N,B)<E(N,A)$ is the desired result for maximum hardness. Therefore, the most-stable state has the maximum chemical hardness.

Finally, note that the Mulliken electronegativity,[31,32] $\chi=\frac{1}{2}(I+A)$, for the ground and excited state will be equal because these states form the same ions. This is the reason for the symmetric appearance of the eigenvalue plots shown throughout Sec. IV.

While we have considered only the exact density functional so far, the lowest HOMO, highest LUMO, and maximum-hardness stability principles will still be shown to hold for approximate functionals. We will consider both the popular B3LYP functional[23,24] and its modified, range-separated variant rCAM-B3LYP,[21,33] which was designed to give improved straight-line behavior for fractional electron numbers. The beryllium cation, the carbon and vanadium atoms, as well as the CH_2 (Ref. 34) and C_3H_3 (Ref. 35) molecules, are considered as illustrative examples. These particular species were chosen since they all have a low-energy excited state and DFT methods predict the correct ground-state configuration.

III. DETAILS OF THE THEORY

The piecewise-linearity condition for the exact functional was originally developed for ground states of fractional charges,[17] fractional spins,[30,36] and combined fractional charge and spins.[37] In this section, we extend this exact condition to a system in the lowest-energy state of a given spin or spatial symmetry. While the fundamental theorems of DFT have been established for ground electronic states, there exists a straightforward extension to a certain class of excited states, the lowest-energy states of a given spin symmetry of the electron density.[15,38–41] Such an extension can also be made to the lowest-energy state of a given spatial symmetry.

We follow the methodology of Yang *et al.*[30] and Mori-Sánchez and co-workers,[36,37] by examining systems at their dissociation limit. Consider an external potential $v(\mathbf{r})$ that has two sets of degenerate states: an N-electron degenerate lowest-energy state of given symmetry S with the energy $E_v^S(N)$, wave functions $(\Phi_{N,i}^S, i=1,2,\ldots,g_N)$ and densities $(\rho_{N,i}^S, i=1,2,\ldots,g_N)$, and a $(N+1)$-electron degenerate lowest-energy state of given symmetry S' with the energy $E_v^{S'}(N+1)$, wave functions $(\Phi_{N+1,j}^{S'}, j=1,2,\ldots,g_{N+1})$ and densities $(\rho_{N+1,j}^{S'}, j=1,2,\ldots,g_{N+1})$. There is an important condition: the two states with symmetry S and S' have to be connected by the addition/removal of one single electron. For example, if we consider the lowest-energy singlet state of the N-electron state, then the $N+1$ state cannot be a quartet state, because these two states cannot be connected by the addition or the removal of a single electron. For the density $\rho=\Sigma_{i=1}^{g_N} c_i \rho_{N,i}^S + \Sigma_{j=1}^{g_{N+1}} d_j \rho_{N+1,j}^{S'}$ where $\{c_i\}$ and $\{d_j\}$ are positive and finite integers, and satisfy the normalization condition, the exact energy functional satisfies the following equation:

$$E_v\left[\frac{1}{q}\sum_{i=1}^{g_N} c_i \rho_{N,i}^S + \frac{1}{q}\sum_{j=1}^{g_{N+1}} d_j \rho_{N+1,j}^{S'}\right] = \frac{q-p}{q} E_v^S(N) + \frac{p}{q} E_v^{S'}(N+1), \tag{18}$$

where $q=\Sigma_{i=1}^{g_N} c_i + \Sigma_{j=1}^{g_{N+1}} d_j$, $p=\Sigma_{j=1}^{g_{N+1}} d_j$, and $q-p=\Sigma_{i=1}^{g_N} c_i$. Equation (18) is our general result on the fractional-charge and fractional-spin condition for systems in the lowest-energy states of given spin and spatial symmetries of the electron density. Equation (18) is also valid in first-order reduced density-matrix functional theory.

We now prove it. Consider a supramolecular system, the following external potential $v_{\mathrm{total}}(\mathbf{r})=\Sigma_{l=1}^{q} v(\mathbf{r}-\mathbf{R}_l)$; namely, it has q copies of the potential $v(\mathbf{r})$, each located at a site $\mathbf{R}_l$ and infinitely far from each other. There is a total number of electrons of $qN+p$ (N, p, and q are all positive and finite integers and $q>p$). Since the sites are separated by infinite

distances, the total system is simply composed of q subsystems in identical external potentials $v(\mathbf{r})$ with no interaction between the subsystems. Its lowest-energy state has $(q-p)$ N-electron subsystems with energy $E_v^S(N)$, which is the N-electron lowest-energy state of the given symmetry S, and p $(N+1)$-electron subsystems with energy $E_v^{S'}(N+1)$, which is the $(N+1)$-electron lowest-energy state of the given symmetry S'.

Note that our results are applicable if and only if the convexity condition,

$$E_v^S(N) \leq (E_v^{S'}(N+1) + E_v^{S''}(N-1))/2, \tag{19}$$

is assumed to hold. This is known for atoms and molecules in their ground states from experimental data[17,19] and is expected to be valid for low-lying excited states. However, this condition is not true for all excited states. For example, the lowest-energy excited state of the lithium cation $(1s2s)$ should autoionize to give the ground states of neutral lithium $(1s^22s)$ and its dication $(1s)$. Given the convexity condition, then the lowest-energy state of the total system is degenerate and its energy is

$$(q-p)E_v^S(N) + pE_v^{S'}(N+1). \tag{20}$$

The total wave function is an antisymmetric product of q separated wave functions. One possible state is the following. For the first p locations, $\mathbf{R}_1 \cdots \mathbf{R}_p$, each has $(N+1)$ electrons; within these p locations, the first d_1 sites have the degenerate wave function $\Phi_{N+1,1}$, the second d_2 sites have the degenerate wave function $\Phi_{N+1,2}^{S'}, \ldots$, and the last $d_{g_{N+1}}$ sites have the degenerate wave function $\Phi_{N+1,g_{N+1}}^{S'}$. In this way, $p=\Sigma_{j=1}^{g_{N+1}} d_j$. For the remaining $q-p$ locations, $\mathbf{R}_{p+1} \cdots \mathbf{R}_q$, each has N electrons; within these $q-p$ locations, the first c_1 sites have the degenerate wave function $\Phi_{N,1}^S$, the second c_2 sites have the degenerate wave function $\Phi_{N,2}^S, \ldots$ and the last c_{g_N} sites have the degenerate wave function Φ_{N,g_N}^S. In this way, $q-p=\Sigma_{i=1}^{g_N} c_i$. Then this state has the wave function

$$\begin{aligned}\Psi_1 = \hat{A}\{&\Phi_{N+1,1}^{S'}(\mathbf{R}_1) \cdots \Phi_{N+1,1}^{S'}(\mathbf{R}_{d_1})\Phi_{N+1,2}^{S'}(\mathbf{R}_{\mathbf{d_1+1}}) \cdots \Phi_{N+1,2}^{S'} \\ &\times(\mathbf{R}_{d_1+d_2}) \cdots \Phi_{N,1}^S(\mathbf{R}_{p+1}) \cdots \Phi_{N,1}^S(\mathbf{R}_{p+c_1})\Phi_{N,2}^S \\ &\times(\mathbf{R}_{p+c_1+1}) \cdots \Phi_{N+1,2}^{S'}(\mathbf{R}_{p+c_1+c_2}) \cdots\}.\end{aligned} \tag{21}$$

The permutation of any two locations with different states $(\Phi_{N,i}^S$ or $\Phi_{N+1,j}^{S'})$ generates a different $(qN+p)$-electron wave function. There are a total of $m=q!/\Pi_i^{g_N} c_i! \Pi_j^{g_{N+1}} d_j!$ such degenerate wave functions.

For any wave function Ψ_k, a particular site $\mathbf{R}_l$ can either have the wave function $\Phi_{N,i}^S$ or $\Phi_{N+1,j}^{S'}$. In all such wave functions $\{\Psi_k, k=1,\ldots,m\}$, the number of times any location $\mathbf{R}_s$ has the wave function $\Phi_{N+1,n}^{S'}$ is equal to $m_{N+1,n} = (q-1)!/(c_n-1)! \Pi_{i\neq n}^{g_N} c_i! \Pi_j^{g_{N+1}} d_j! = mc_n/q$ and the corresponding number for $\Phi_{N,n}^S$ is equal to $m_{N,n}=(q-1)!/(d_n-1)! \Pi_i^{g_N} c_i! \Pi_{j\neq n}^{g_{N+1}} d_j! = md_n/q$. In analogy to Eq. (21), the following equally weighted wave function is also a degenerate wave function:

$$\bar{\Psi} = \frac{1}{\sqrt{m}} \sum_{k=1}^{m} \Psi_k, \tag{22}$$

the density of which is

$$\bar{\rho} = \sum_{l=1}^{q} \left(\frac{1}{q} \sum_{i=1}^{g_N} c_i \rho_{N,i}^S(\mathbf{R}_l) + \frac{1}{q} \sum_{j=1}^{g_{N+1}} d_j \rho_{N+1,j}^{S'}(\mathbf{R}_l) \right). \tag{23}$$

In this particular state with the degenerate energy of Eq. (20), all the q subsystems have the same electron density except by translation. For the exact functional, it must be size-extensive $E_v[\bar{\rho}] = qE_v[(1/q)\Sigma_{i=1}^{g_N} c_i \rho_{N,i}^S(\mathbf{R}_l) + (1/q)\Sigma_{j=1}^{g_{N+1}} d_j \rho_{N+1,j}^{S'}(\mathbf{R}_l)]$. However, $E_v[\bar{\rho}] = (q-p)E_v^S(N) + pE_v^{S'}(N+1)$ according to Eq. (20). Therefore, we have

$$\begin{aligned}&E_v\left[\frac{1}{q} \sum_{i=1}^{g_N} c_i \rho_{N,i}^S(\mathbf{R}_l) + \frac{1}{q} \sum_{j=1}^{g_{N+1}} d_j \rho_{N+1,j}^{S'}(\mathbf{R}_l) \right] \\ &\quad = \frac{q-p}{q} E_v^S(N) + \frac{p}{q} E_v^{S'}(N+1),\end{aligned} \tag{24}$$

which is just Eq. (18), for the site $\mathbf{R}_l$. It is the size-extensivity requirement that leads to the definition of energy for densities with fractional charges and spins in Eq. (24).

Note that since in Eq. (18), the energy functional is for the lowest-energy state of some given symmetry, there is no spin contamination problem[42,43] for the functional so defined. In other words, such functionals are symmetry specific.

IV. RESULTS AND DISCUSSION

A. Be atom

As a simple example, we first consider the beryllium atom, which has a ground-state electronic configuration of $1s^22s^2$. There is also a low-lying triplet excited state with configuration $1s^22s^12p^1$. Ionization from this excited state can give two low-energy cations: the ground-state $(1s^22s^1)$ or the first excited state $(1s^22p^1)$. Further ionization gives a common dication with configuration $1s^2$. This situation is illustrated by the $E(N)$ curve in Fig. 2.

This curve was generated from calculations with the rCAM-B3LYP[21,33] functional and the cc-pVQZsdp basis set (cc-pVQZ with only s, p, and d functions) using the CADPAC program.[44] Energies were calculated as a function of (fractional) electron number for each ionization process. Figure 2 also shows the eigenvalues of the relevant orbitals involved in each ionization. These (generalized Kohn–Sham) eigenvalues correspond to the slopes of the $E(N)$ curves.

This plot can be used to compare the properties of the two cation states. The $1s^22s^1$ cation is the ground state and has the most-stable HOMO. Only the excited-state $1s^22s^12p^1$ neutral can be reached from both cations via one-electron processes. This state is generated by an electron addition to an s orbital of the $1s^22p^1$ cation or to a p orbital of the $1s^22s^1$ cation. Comparing these unoccupied orbital eigenvalues, that of the ground-state is higher in energy. Combining these results, the ground-state cation has the largest energy gap and chemical hardness.

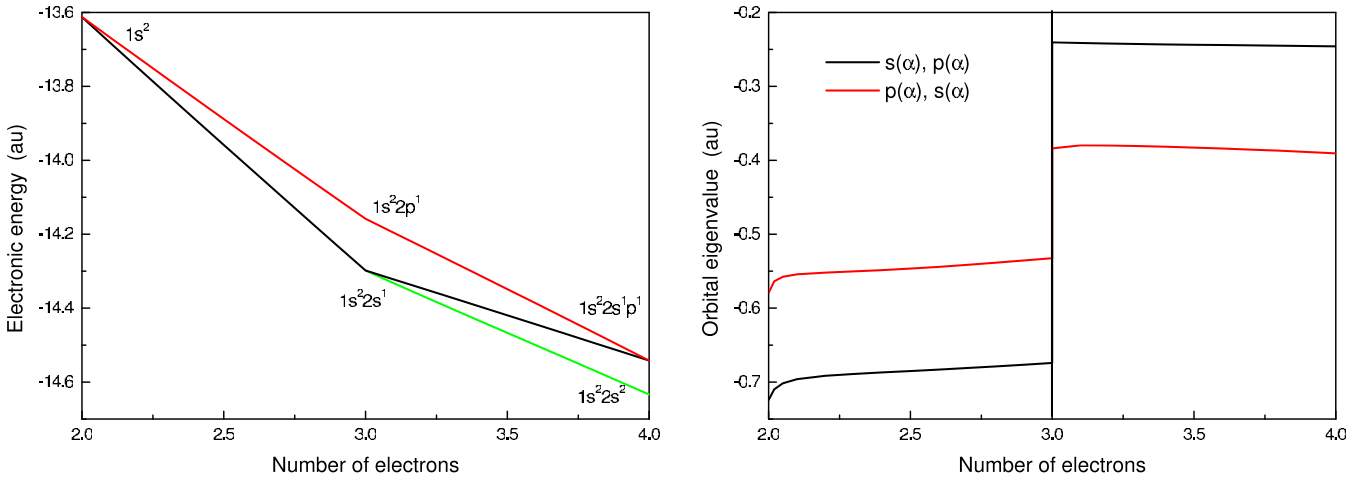

FIG. 2. Electronic energies and orbital eigenvalues of the beryllium atom as a function of the number of electrons. An ordinate value of 2.0 corresponds to the dication, 3.0 the cation, and 4.0 the neutral atom. The ground-state cation has the $1s^2 2s^1$ configuration. The eigenvalues are the slopes of the $E(N)$ curves and represent the HOMO and LUMO/LUMO+1 of the cation states.

B. C atom

The next example is the carbon atom, which has an electronic configuration of $1s^2 2s^2 2p^2$. The ground state is a triplet (^{3}P) with the two p electrons unpaired. There is also a low-lying singlet excited state (^{1}D). This example is complicated by the fact that this state is an open-shell singlet, the energy of which cannot be obtained using a single Slater determinant reference state with currently available functionals. Ionization of either the singlet or triplet neutral gives the ground-state doublet (^{2}P) cation. The electron addition to both neutral states can give a common doublet anion. However, this state is again not representable as a single determinant and will be higher in energy than the ground-state quartet (^{4}S) anion.

In this work, rCAM-B3LYP/cc-pVQZsdp calculations were performed for the lowest-energy single determinants. These are $p_x(\alpha)$ for the dication, $p_x(\alpha)p_y(\alpha)$ for the triplet neutral, $p_x(\alpha)p_z(\beta)$ for the singlet neutral, $p_x(\alpha)p_y(\alpha)p_z(\alpha)$ for the quartet anion, and $p_x(\alpha)p_y(\alpha)p_z(\beta)$ for the doublet anion. The energy difference between the lowest single-determinant singlet and triplet states of neutral carbon was calculated to be 3649 cm^{-1}. However, this actually corresponds to half of the ^{1}D-^{3}P splitting. Employing the correction of Ziegler *et al.*[42] gives improved agreement with the experimental value of 10 160 cm^{-1}.[45]

Figure 3 shows $E(N)$ curves calculated for ionization from, or electron addition to, both the singlet and triplet states of the neutral carbon atom. The figure also shows the relevant orbital eigenvalues as a function of an electron number, $\varepsilon(N)$, which corresponds to the slopes of the $E(N)$ curves.

The calculated eigenvalues clearly show that the ground-state, triplet neutral has the most-stable HOMO. The ground-state anion is the quartet, which cannot be reached from the singlet neutral by a one-electron process. To directly compare the two neutral states, the shared, doublet anion must be considered. This state can be reached by addition of an α-spin electron to the singlet neutral or a β-spin electron to the triplet neutral. Comparing these unoccupied orbital eigenvalues, that of the triplet is higher in energy, again indi-

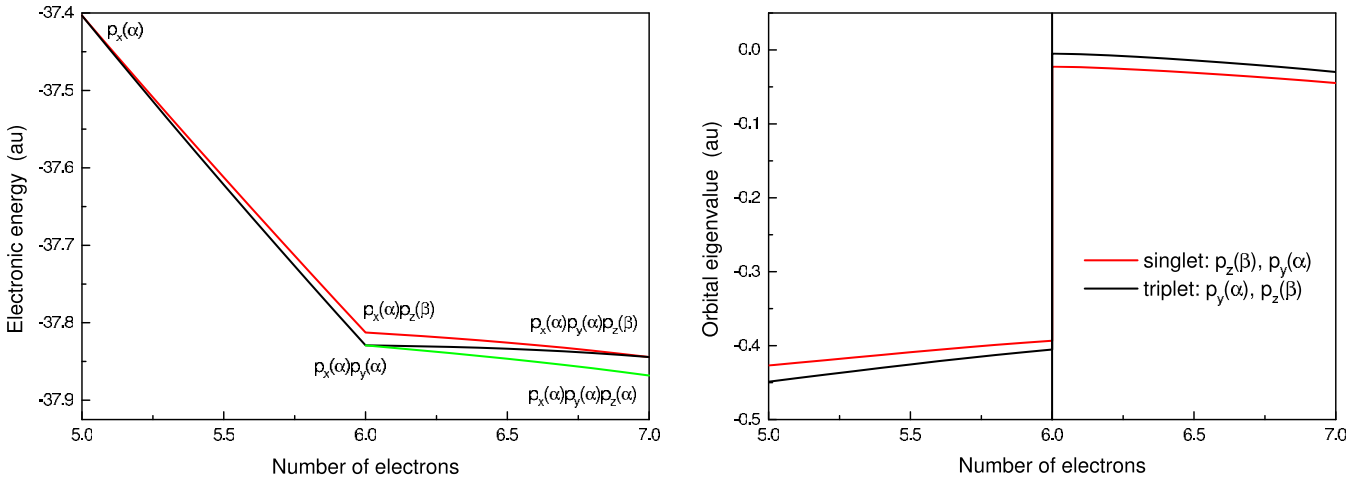

FIG. 3. Electronic energies and orbital eigenvalues of the carbon atom as a function of the number of electrons. An ordinate value of 5.0 corresponds to the cation, 6.0 the neutral atom, and 7.0 the anion. Calculations were performed for the lowest-energy single determinants. The ground-state neutral is the triplet $[p_x(\alpha)p_y(\alpha)]$. The eigenvalues are the slopes of the $E(N)$ curves and represent the HOMO and LUMO/LUMO+1 of the neutral states.

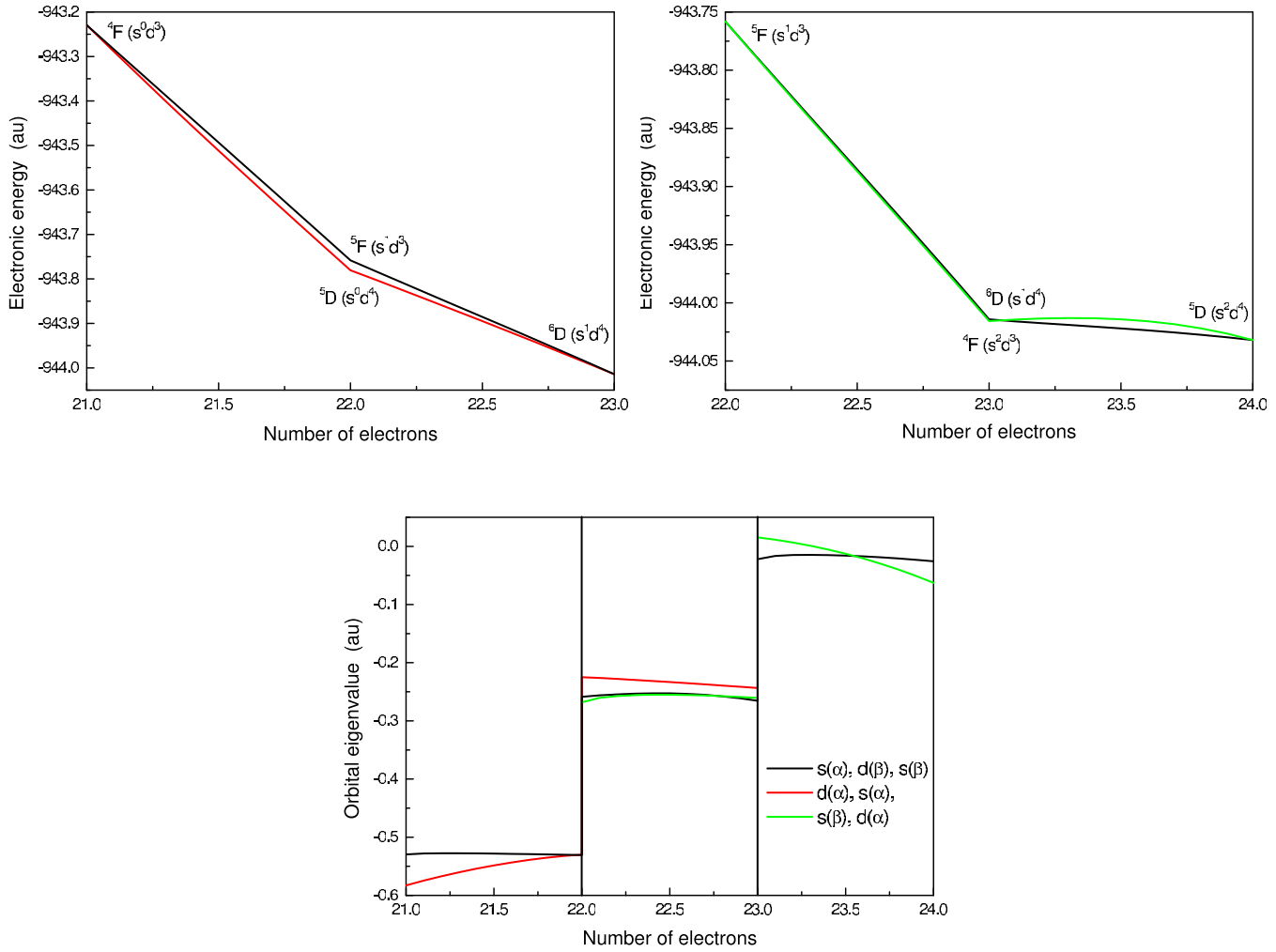

FIG. 4. Electronic energies and orbital eigenvalues of the vanadium atom as a function of the number of electrons. An ordinate value of 21.0 corresponds to the dication, 22.0 the cation, 23.0 the neutral atom, and 24.0 the anion. The ground-state cation is ^{5}D and the ground-state neutral is ^{4}F.

cating that it is the neutral ground state. Taken together, the triplet also has the largest energy gap and chemical hardness.

C. V atom

In this section, we consider the more complex example of the vanadium atom, which has several low-lying electronic states. The ground state has a ^{4}F electronic configuration of s^2d^3. It is only 0.11 eV or 2.5 kcal/mol lower in energy[46] than the lowest excited state, which has a ^{6}D electronic configuration of s^1d^4. Electron addition to these two neutral states gives the ground-state ^{5}D anion (s^2d^4). Ionization from the HOMO of the ^{6}D neutral gives the ground-state ^{5}D cation (s^0d^4). However, this cation cannot be reached from the ground-state ^{4}F neutral by a one-electron process. Ionization from this neutral gives instead the lowest excited state cation, which has an ^{5}F electronic configuration of s^1d^4. This ^{5}F cation can also be reached from the ^{6}D neutral by ionization from the s-orbital. Further ionization from either cation gives the same ^{4}F dication (s^0d^3).

This collection of states is illustrated in the two $E(N)$ curves in Fig. 4. The calculations were performed in the same manner as for beryllium and carbon using the rCAM-B3LYP[21,33] functional and the cc-pVQZsdp basis set.[44] The choice of d orbital occupations was made according to Ref. 47. Figure 4 also plots $\varepsilon(N)$ for each ionization or electron addition process.

Let us begin with the more straightforward case of the ^{5}D and ^{5}F cation states, which are connected by one-electron processes with the dication and ^{6}D neutral. The eigenvalues show that the ground-state ^{5}D cation has the lower HOMO, higher LUMO, greater energy gap, and thus maximum chemical hardness. Comparison of the two neutral states is more difficult. They are connected by one-electron processes with the ^{5}F cation and the anion. However, Fig. 4 shows that the $E(N)$ curves for formation of the ^{5}F cation from either neutral are essentially superimposed and, consequently, that HOMO eigenvalues are nearly degenerate. Moreover, no definitive conclusions can be drawn from a comparison of the LUMO eigenvalues due to the substantial curvature of the calculated $E(N)$ curve for electron addition to the ^{4}F neutral (caused by delocalization error, indicating that a different range-separation may be needed in rCAM-B3LYP for d orbitals). That the HOMO and LUMO eigenvalues of these two neutral states are nearly degenerate or cross, with approximate functionals, is of no surprise due to the very small calculated energy difference of 1.0 kcal/mol between them.

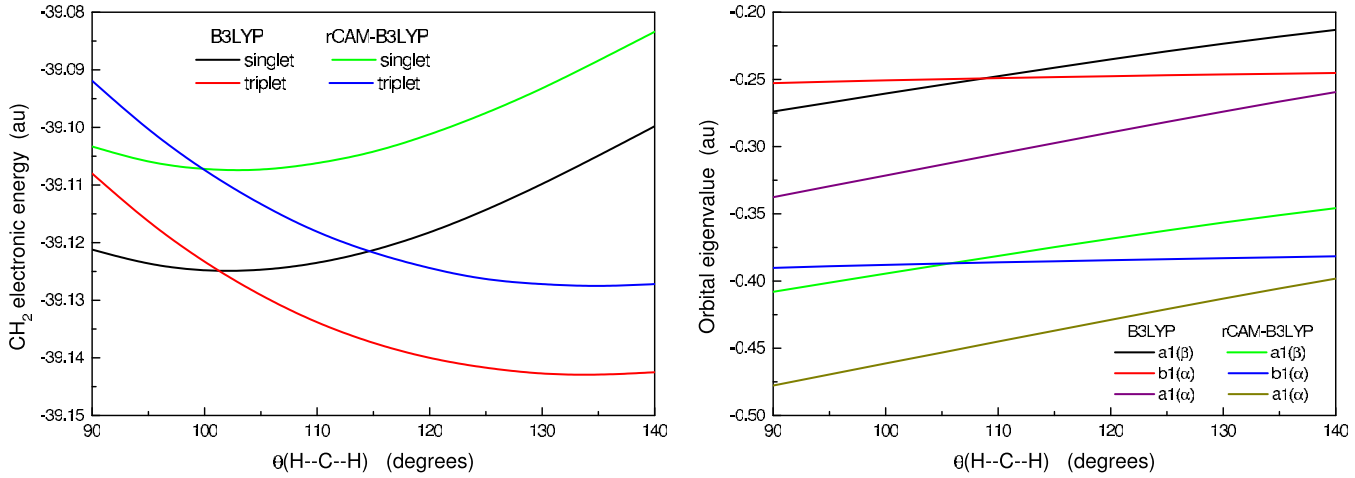

FIG. 5. Total electronic energies and orbital eigenvalues of CH_2 as a function of angle. The orbital eigenvalues correspond to the HOMO-1 [a1(α)] singlet-state HOMO [a1(β)] and triplet-state HOMO [b1(α)].

D. CH_2

The next example is the CH_2 molecule, which has been the subject of highly advanced correlated wave function studies.[34] In this molecule, there are two electrons on the carbon atom not directly involved in chemical bonding. These electrons can share occupancy of an a1 orbital, resulting in a singlet (1-A1) state. Alternatively, the molecule can adopt a triplet (3-B1) state with same-spin electrons occupy-

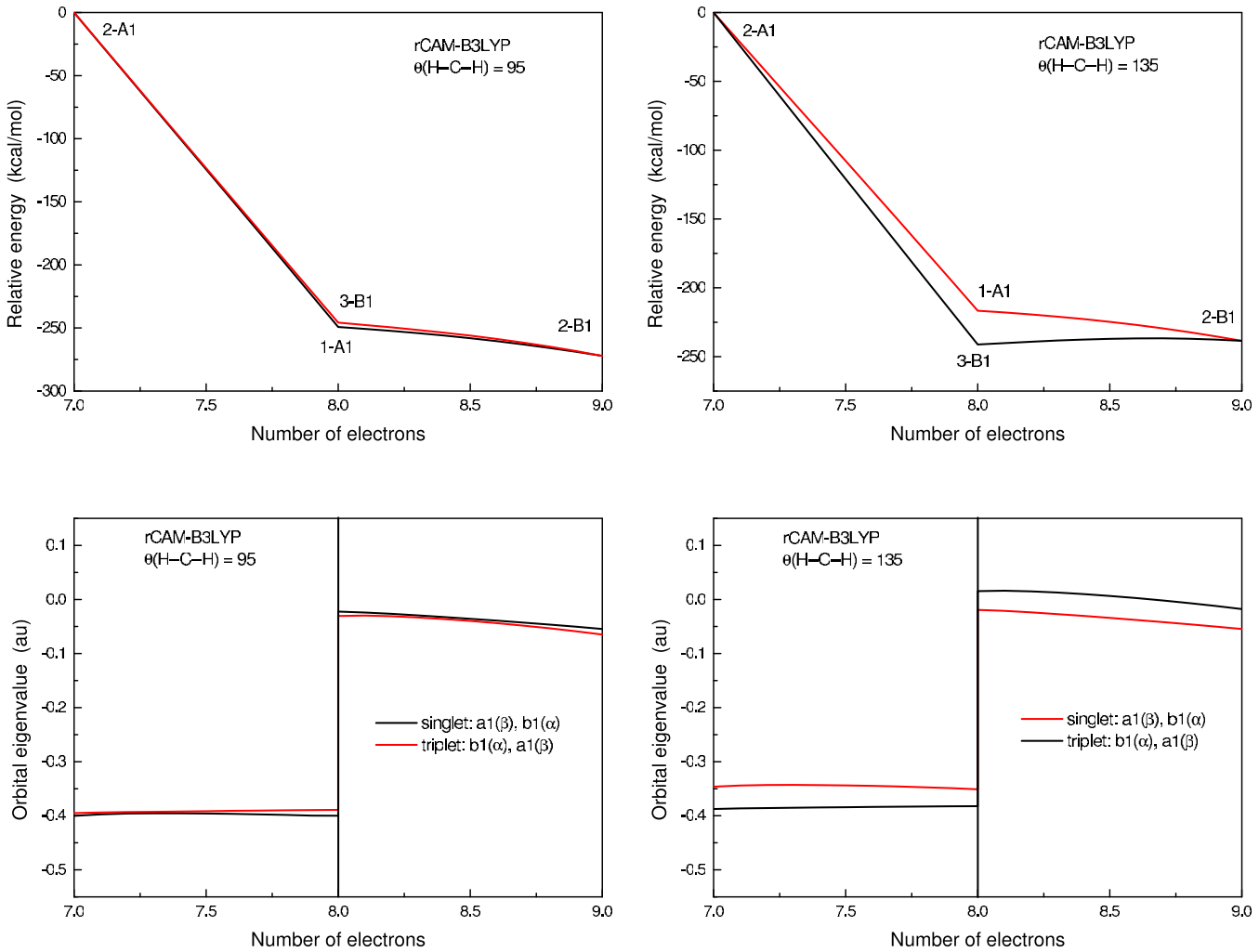

FIG. 6. rCAM-B3LYP relative electronic energies and orbital eigenvalues of CH_2 as a function of the number of electrons. An ordinate value of 7.0 corresponds to the cation, 8.0 the neutral molecule, and 9.0 the anion. Results are shown for two molecular geometries with angles of 95° (left) and 135° (right).

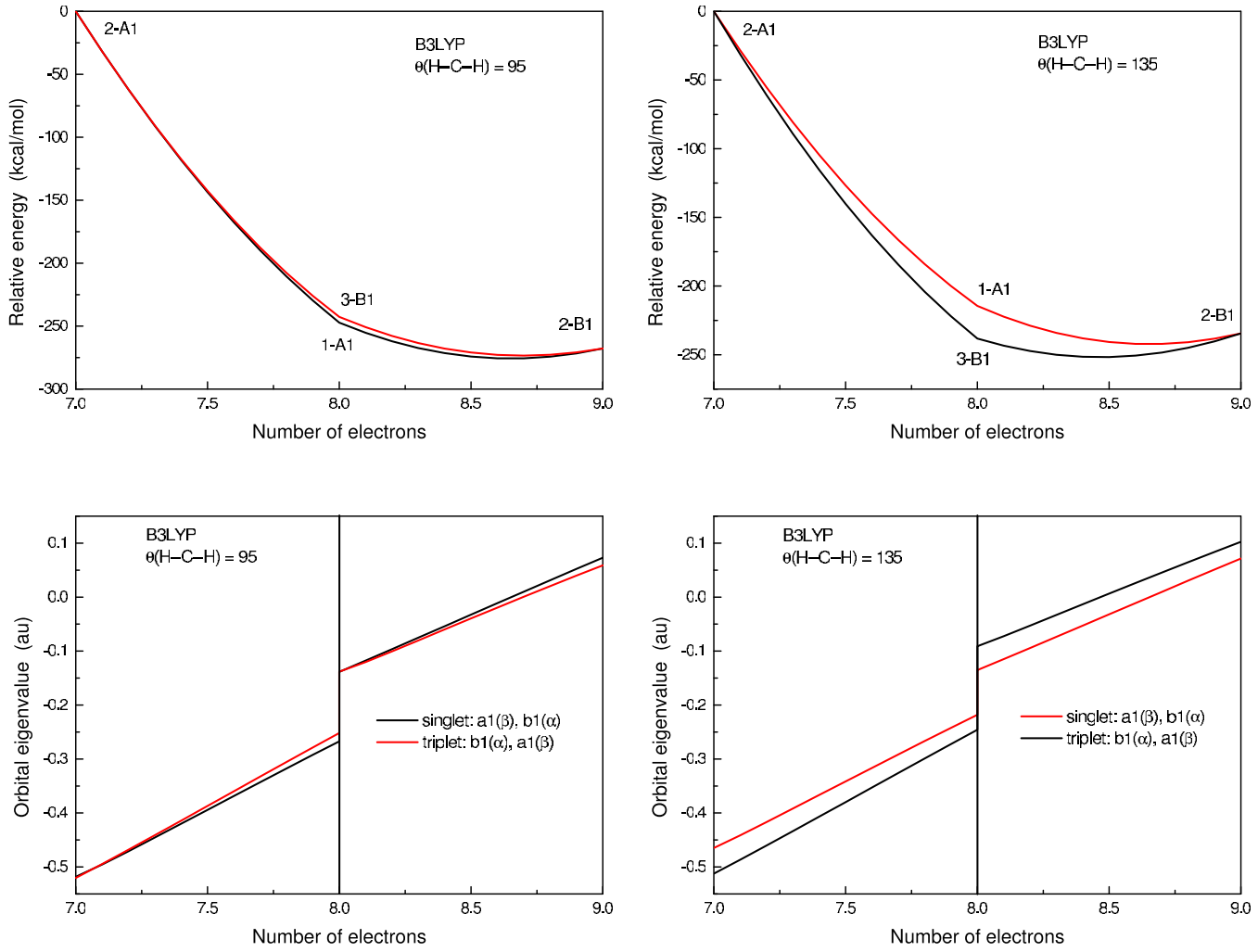

FIG. 7. B3LYP relative electronic energies and orbital eigenvalues of CH_2 as a function of the number of electrons. An ordinate value of 7.0 corresponds to the cation, 8.0 the neutral molecule, and 9.0 the anion. Results are shown for two molecular geometries with angles of 95° (left) and 135° (right).

ing the a1 and b1 orbitals. The energy ordering of the singlet and triplet states changes as a function of the H–C–H angle.[34]

In our calculations, the two C–H bonds were fixed at R(C–H)=1.1 Å. The H–C–H angle was varied between 90° and 140° in 5° increments. At each of these geometries, single point energy calculations were performed with the rCAM-B3LYP[21,33] and B3LYP[23,24] functionals using the cc-pVQZsdp basis set.[44]

The resulting potential-energy curves as a function of H–C–H angle are shown in Fig. 5. The figure also shows a Walsh-type diagram, plotting the orbital eigenvalues as a function of angle. The two functionals provide very similar results. The 1-A1 state is more stable at small angles, while the minimum-energy geometry is obtained with the 3-B1 state at larger angles. The singlet and triplet are degenerate at approximately 102°. Of the three orbital eigenvalues plotted, the occupied HOMO-1 a1(α) is consistently lowest in energy. The HOMO can be either an a1(β) orbital in the singlet or a b1(α) orbital in the triplet. The a1(β) eigenvalue is lower at small angles, where the singlet state is more stable, and the b1(α) eigenvalue is lower at large angles, where the triplet state is more stable. The orbital eigenvalues show that the most-stable configuration has the lowest HOMO energy and highest LUMO energy. The a1(β) and b1(α) eigenvalues become degenerate at approximately 107°, which is somewhat larger than the crossing point in the potential-energy curves. At this crossing point, the HOMO and LUMO eigenvalues for both states are equal and the band-gap is zero.

We now select two CH_2 geometries with angles of 95° and 135°. $E(N)$ curves were calculated for ionization from the HOMO or electron addition to the LUMO of both the singlet and triplet states. The results for both geometries are shown in Fig. 6 for rCAM-B3LYP and Fig. 7 for B3LYP. The energies are expressed relative to the cation so that the results from both functionals are directly comparable. Note that ionization from either the neutral singlet or triplet produces the same 2-A1 cation state. Similarly, reduction of either the singlet or triplet gives the same 2-B1 anion state. For the 1-A1 neutral, ionization is from the a1(β) orbital and electron addition is to the b1(α) orbital. Conversely, for the 3-B1 neutral, ionization is from the b1(α) orbital and electron addition is to the a1(β) orbital. Figures 6 and 7 also show plots of $\varepsilon(N)$ for these particular orbital eigenvalues.

The $E(N)$ curves obtained with B3LYP (Fig. 7) are concave, showing the tendency of this functional to overstabilize

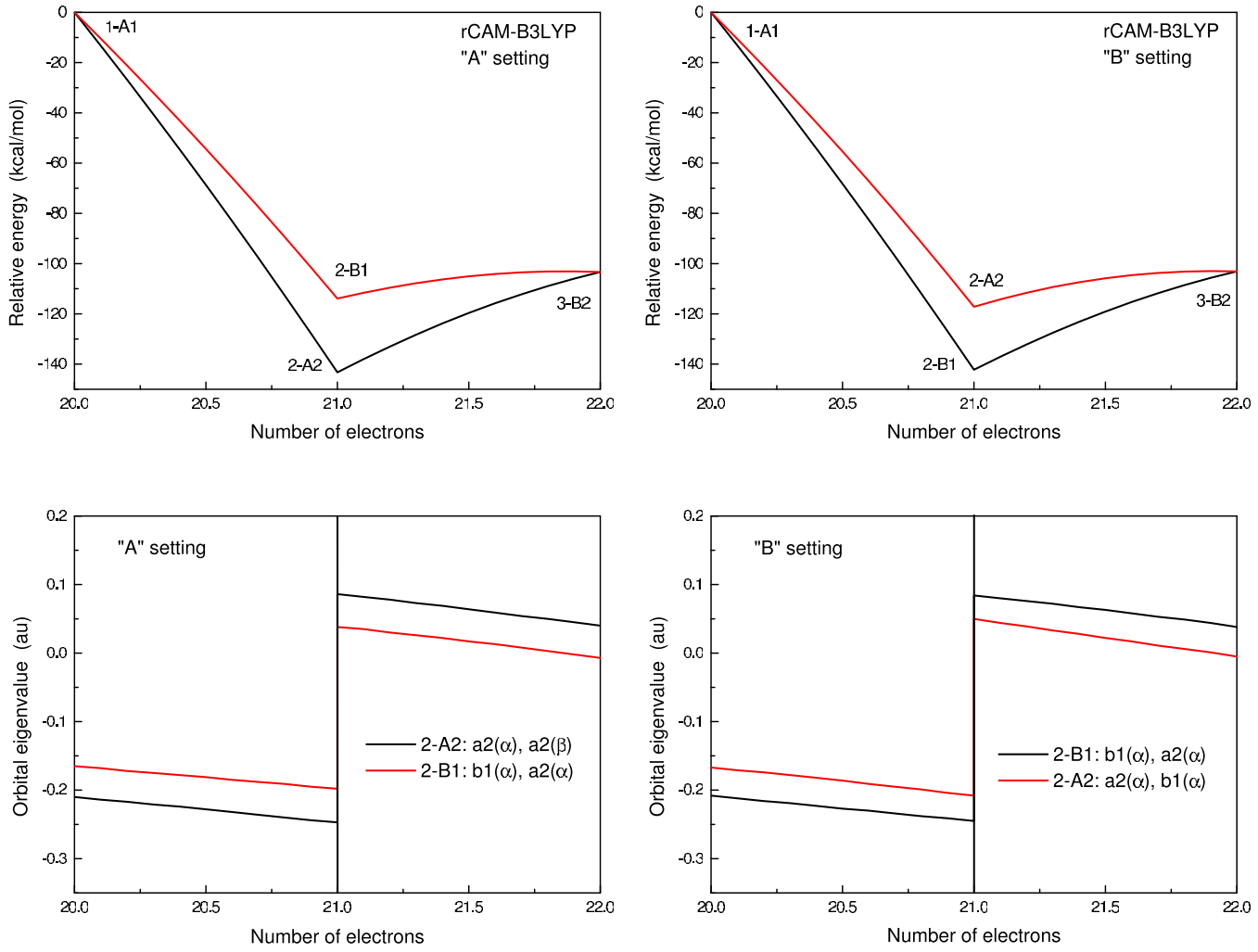

FIG. 8. rCAM-B3LYP relative electronic energies and orbital eigenvalues of C_3H_3 as a function of the number of electrons. An ordinate value of 20.0 corresponds to the cation, 21.0 the neutral molecule, and 22.0 the anion. Results are shown for two molecular geometries.

systems with fractional charges; this is characteristic of delocalization error. Although slightly convex, the rCAM-B3LYP curves (Fig. 6) are more nearly linear since this functional was designed to have reduced delocalization error. The B3LYP eigenvalues increase considerably between the integers to match the concave shape of the $E(N)$ plots. The rCAM-B3LYP eigenvalues are much closer to the constant result expected from the exact functional, but are found to decrease slightly between the integers reflecting the convexity of the $E(N)$ curves.

First consider the CH_2 geometry with an internal angle of 95°. Starting from the ground-state cation, the most-stable neutral will be formed by electron addition to the lowest-energy unoccupied orbital, which is the a1(β) orbital. Thus, the most-stable configuration of the neutral CH_2 molecule at this geometry is 1-A1, which has the lowest-energy HOMO. Conversely, starting from the ground-state anion, the most-stable neutral will be formed by removing an electron from the highest-energy occupied orbital, which is the b1(α) orbital. This again predicts the 1-A1 neutral, which has the highest-energy LUMO, to be most stable. Taken together, these results mean that the most-stable neutral must also have the largest band-gap and consequently the greater chemical hardness.

Now consider the CH_2 geometry with an internal angle of 135°. Starting from the cation, an electron will add to the lowest-energy unoccupied orbital, which is now b1(α). Conversely, starting from the anion, an electron will ionize from the highest-energy occupied orbital, which is now a1(β). Both of these processes give the 3-B1 neutral. The state with the lowest-energy HOMO, highest-energy LUMO, and greatest chemical hardness, is predicted to be most stable.

Note that while CH_2, at equilibrium geometry, has the greatest hardness as a triplet, the analogous molecule CCl_2 has the greatest hardness in its singlet ground state. This demonstrates the transferability of the maximum-hardness principle.

E. C_3H_3

The last test case considered is the C_3H_3 molecule, which has also been the subject of earlier computational studies.[35] While the ground-state 1-A1 cation has D3h symmetry, the neutral molecule is a doublet that undergoes a Jahn–Teller type distortion to give a Cs ground state with two longer C–C bonds and the nonequivalent H atom out of the plane of the molecule. However, there are two previously studied[35] geometries within the C2v point group that we will

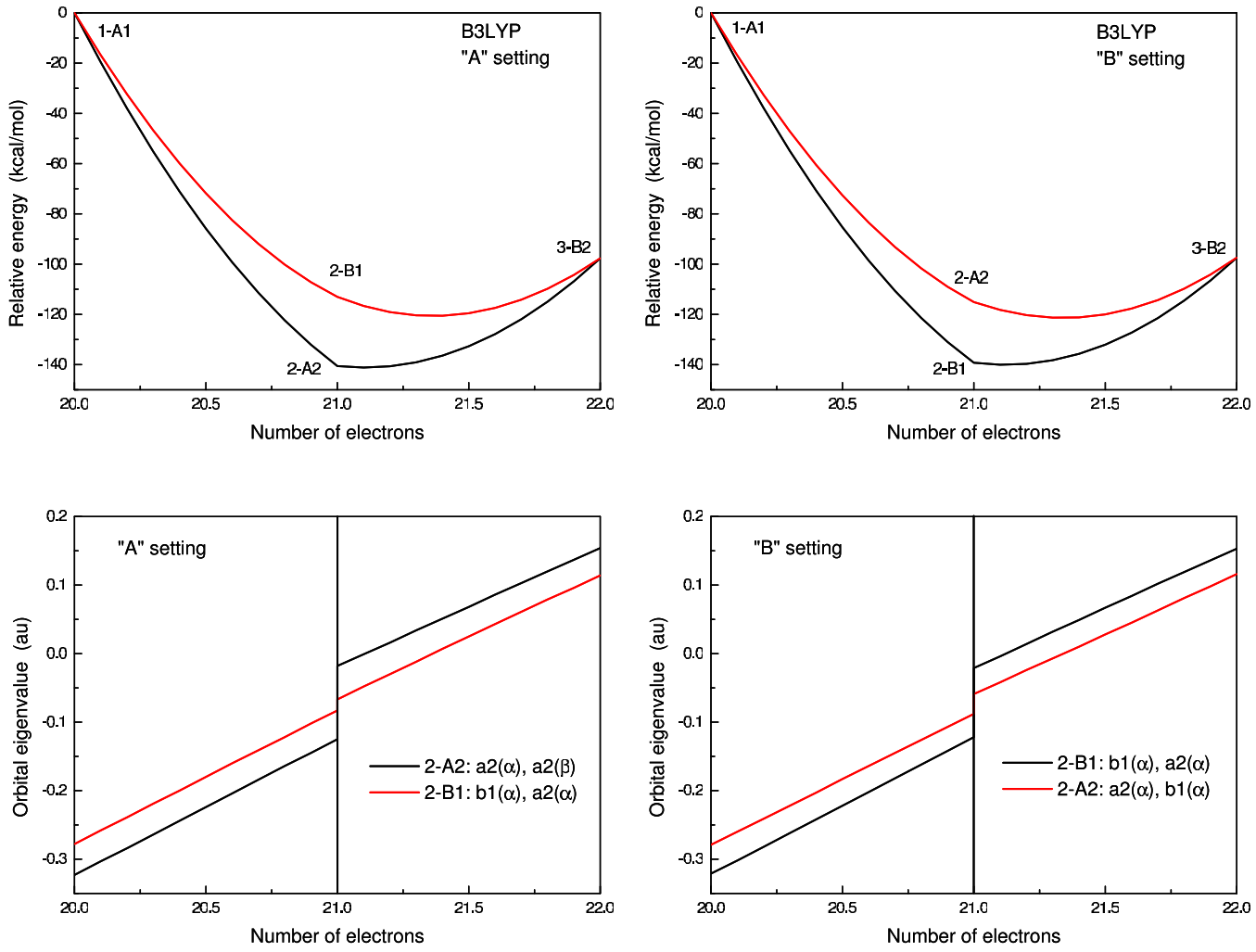

FIG. 9. B3LYP relative electronic energies and orbital eigenvalues of C_3H_3 as a function of the number of electrons. An ordinate value of 20.0 corresponds to the cation, 21.0 the neutral molecule, and 22.0 the anion. Results are shown for two molecular geometries.

consider: the "A setting" (two short C–C bonds) and the "B setting" (two long C–C bonds). The ground electronic state differs between these two geometries: 2-A2 for the A setting and 2-B1 for the B setting. Therefore, the ground and lowest-energy excited states have the same spin but the electron densities have different spatial symmetries.

The C2v geometries of the C_3H_3 molecule were optimized for the A and B settings in their ground-state configurations with B3LYP/cc-pVQZspd using GAUSSIAN 03.[48] These two states are predicted to be nearly degenerate with the B setting slightly more stable by 0.7 kcal/mol. For each geometry, $E(N)$ and $\varepsilon(N)$ curves were generated for both the ground and lowest excited states The results are shown in Fig. 8 for rCAM-B3LYP and Fig. 9 for B3LYP.

Ionization results in a 1-A1 state for the cation in all cases with the electron removed from either the singly occupied a2(α) or b1(α) orbitals. Electron addition is more complex. An α-spin electron can be added to either neutral state to give a 3-B2 anion. Alternatively, two possible 1-A1 anions can be generated from an addition of a β-spin electron. The electron can be added to the 2-A2 neutral to give a HOMO occupation of a2($\alpha\beta$) or to the 2-B1 neutral to give a HOMO occupation of b1($\alpha\beta$). In DFT calculations, the two 1-A1 anions are represented as pure states, while they would mix and give lower energy in a multireference CI treatment. The 3-B2 anion is predicted to be most stable, although the electron affinity is negative when constrained to either neutral geometry. Previous work demonstrated that the optimized anion geometry is highly nonplanar.[49]

Consider the $E(N)$ curves for the two neutral geometries in Fig. 8 obtained with rCAM-B3LYP. In the A setting, the 2-A2 state is lower in energy than the 2-B1 state by 29.4 kcal/mol. Conversely, in the B setting, the 2-B1 state is lower in energy than the 2-A2 state by 25.1 kcal/mol. The $E(N)$ curves are somewhat convex and the eigenvalues (slopes) decrease with increasing electron number N. B3LYP gives the same general pattern of results (see Fig. 9), except that this functional gives highly concave $E(N)$ curves and the eigenvalues increase with increasing N.

Starting from the 1-A1 cation, an electron will add to the lowest-energy orbital. In the A setting, this is the a2(α) orbital to give the 2-A2 neutral. In the B setting, this is the b1(α) orbital to give the 2-B1 neutral. In both cases, the most-stable state must have the lowest HOMO energy. Now consider removing an electron from the highest-energy orbital of the 3-B2 anion. In the A setting, this is the b1(α)

orbital and gives the 2-A2 neutral. In the B setting, this is the a2(α) orbital and gives the 2-B1 neutral. Again, the most-stable neutral state must have the highest LUMO energy. (Note that this analysis would not apply to the singlet anion states, since addition of a β-spin electron to the two neutral configurations does not give the same anion.) Finally, in both settings, the most-stable neutral configuration has the largest HOMO-LUMO gap, and therefore, the largest chemical hardness.

V. SUMMARY AND OUTLOOK

For the exact density functional, we have proven a "flat-plane" condition for the lowest-lying excited states of different spin or spatial symmetry from the ground state. This condition means that the electronic energies must be piecewise linear as a function of fractional charge or fractional spin. As a consequence of this, we have also proven that the most-stable electronic state of an atom or molecule will have the lowest HOMO energy, highest LUMO energy, and maximum chemical hardness. This rigorous maximum-hardness principle directly connects the experimental observables of ionization potential and electron affinity to spin-state energy splittings.

The maximum-hardness principle was demonstrated for the Be, C, and V atoms. Additionally, the examples of the CH_2 and C_3H_3 molecules show that this principle still hold for approximate functionals even with significant delocalization error. The current findings could prove useful in application to compounds such as dyes and electronic materials, which have low-lying excited states. Our maximum-hardness principle for different electronic states can also be combined with the existing result for different geometries. Increases in chemical hardness originating from changes in spin, orbital symmetry, and geometric distortions should all lead to greater stability.

ACKNOWLEDGMENTS

This work is supported by the National Science Foundation (W.Y., Contract No. CHE-06-16849-03).

[1] H. F. Schaefer, Science **231**, 1100 (1986).
[2] K. K. Irikura, W. A. Goddard, and J. L. Beauchamp, J. Am. Chem. Soc. **114**, 48 (1992).
[3] J. Harvey, Struct. Bonding (Berlin) **112**, 151 (2004).
[4] J. L. Carreón-Macedo and J. N. Harvey, Phys. Chem. Chem. Phys. **8**, 93 (2006).
[5] D. A. Scherlis, M. Cococcioni, P. Sit, and N. Marzari, J. Phys. Chem. B **111**, 7384 (2007).
[6] A. D. Walsh, J. Chem. Soc. **1953**, 2260 (1953).
[7] C. A. Coulson and B. M. Deb, Int. J. Quantum Chem. **5**, 411 (1971).
[8] N. H. March, J. Chem. Phys. **74**, 2973 (1981).
[9] R. G. Pearson, Acc. Chem. Res. **26**, 250 (1993).
[10] R. G. Parr and R. G. Pearson, J. Chem. Soc. **105**, 7512 (1983).
[11] P. K. Chattaraj, S. Nath, and A. B. Sannigrahi, Chem. Phys. Lett. **212**, 223 (1993).
[12] M. K. Harbola, Proc. Natl. Acad. Sci. U.S.A. **89**, 1036 (1992).
[13] R. G. Parr and P. K. Chattaraj, J. Am. Chem. Soc. **113**, 1854 (1991).
[14] P. W. Ayers and R. G. Parr, J. Am. Chem. Soc. **122**, 2010 (2000).
[15] R. G. Parr and W. Yang, *Density-Functional Theory of Atoms and Molecules* (Oxford University Press, New York, 1989).
[16] R. G. Parr, R. A. Donnelly, M. Levy, and W. E. Palke, J. Chem. Phys. **68**, 3801 (1978).
[17] J. P. Perdew, R. G. Parr, M. Levy, and J. L. Balduz, Phys. Rev. Lett. **49**, 1691 (1982).
[18] J. F. Janak, Phys. Rev. B **18**, 7165 (1978).
[19] Z. Zhou and R. G. Parr, J. Am. Chem. Soc. **111**, 7371 (1989).
[20] A. Seidl, A. Gorling, P. Vogl, J. A. Majewski, and M. Levy, Phys. Rev. B **53**, 3764 (1996).
[21] A. J. Cohen, P. Mori-Sánchez, and W. Yang, J. Chem. Phys. **126**, 191109 (2007).
[22] W. Yang, P. W. Ayers, and Q. Wu, Phys. Rev. Lett. **92**, 146404 (2004).
[23] A. D. Becke, J. Chem. Phys. **98**, 5648 (1993).
[24] C. Lee, W. Yang, and R. G. Parr, Phys. Rev. B **37**, 785 (1988).
[25] A. J. Cohen, P. Mori-Sánchez, and W. Yang, J. Chem. Theory Comput. **5**, 786 (2009).
[26] Y. Zhang and W. Yang, J. Chem. Phys. **109**, 2604 (1998).
[27] A. J. Cohen, P. Mori-Sánchez, and W. Yang, Phys. Rev. B **77**, 115123 (2008).
[28] P. Mori-Sánchez, A. J. Cohen, and W. Yang, Phys. Rev. Lett. **100**, 146401 (2008).
[29] A. J. Cohen, P. Mori-Sánchez, and W. Yang, Science **321**, 792 (2008).
[30] W. Yang, Y. Zhang, and P. W. Ayers, Phys. Rev. Lett. **84**, 5172 (2000).
[31] R. S. Mulliken, J. Chem. Phys. **3**, 573 (1935).
[32] R. G. Pearson, J. Am. Chem. Soc. **107**, 6801 (1985).
[33] T. Yanai, D. P. Tew, and N. C. Handy, Chem. Phys. Lett. **393**, 51 (2004).
[34] J. R. Flores and R. J. Gdanitz, J. Chem. Phys. **123**, 144316 (2005).
[35] E. R. Davidson and W. T. Borden, J. Chem. Phys. **67**, 2191 (1977).
[36] A. J. Cohen, P. Mori-Sánchez, and W. Yang, J. Chem. Phys. **129**, 121104 (2008).
[37] P. Mori-Sánchez, A. J. Cohen, and W. Yang, Phys. Rev. Lett. **102**, 066403 (2009).
[38] O. Gunnarsson and B. I. Lundqvist, Phys. Rev. B **13**, 4274 (1976).
[39] U. von Barth, Phys. Rev. A **20**, 1693 (1979).
[40] H. Englisch and R. Englisch, Physica A **121**, 253 (1983).
[41] F. W. Kutzler and G. S. Painter, Phys. Rev. Lett. **59**, 1285 (1987).
[42] T. Ziegler, A. Rauk, and E. J. Baerends, Theor. Chim. Acta **43**, 261 (1977).
[43] J. Baker, A. Scheiner, and J. Andzelm, Chem. Phys. Lett. **216**, 380 (1993).
[44] R. D. Amos, I. L. Alberts, J. S. Andrews, S. M. Colwell, N. C. Handy, D. Jayatilaka, P. J. Knowles, R. Kobayashi, K. E. Laidig, G. Laming, A. M. Lee, P. E. Maslen, C. W. Murray, J. E. Rice, E. D. Simandiras, A. J. Stone, M.-D. Su, and D. J. Tozer, CADPAC6.5, the Cambridge analytic derivatives package, 1998.
[45] C. E. Moore, *Atomic Energy Levels*, Natl. Bur. Stand. (U.S.) Circ. No. 467 (U.S. GPO, Washingston, DC, 1949).
[46] K. Raghavachari and G. W. Trucks, J. Chem. Phys. **91**, 1062 (1989).
[47] E. R. Johnson, R. M. Dickson, and A. D. Becke, J. Chem. Phys. **126**, 184104 (2007).
[48] M. J. Frisch, G. W. Trucks, H. B. Schlegel *et al.*, GAUSSIAN 03, Revision C.02, Gaussian, Inc., Wallingford, CT, 2004.
[49] G. N. Merrill and S. R. Kass, J. Am. Chem. Soc. **119**, 12322 (1997).